Supplementary Material (ESI) for Journal of Materials Chemistry

Supporting Information

Synthesis and FET characteristics of phenylene-vinylene and anthracene-vinylene compounds containing cyano groups

Kohei Shoji,[a] Jun-ichi Nishida,[a] Daisuke Kumaki[b]
Shizuo Tokito[b] and Yoshiro Yamashita*[a]

[a]Department of Electronic Chemistry, Interdisciplinary Graduate School of Science and Engineering, Tokyo Institute of Technology, Nagatsuta, Midori-ku, Yokohama 226-8502, *Japan*.
[b]NHK Science and Technical Research Laboratories, Kinuta, Setagaya-ku, Tokyo 157-8510, *Japan*.

E-mail: yoshiro@echem.titech.ac.jp

Contents

1. Differential pulse voltammograms

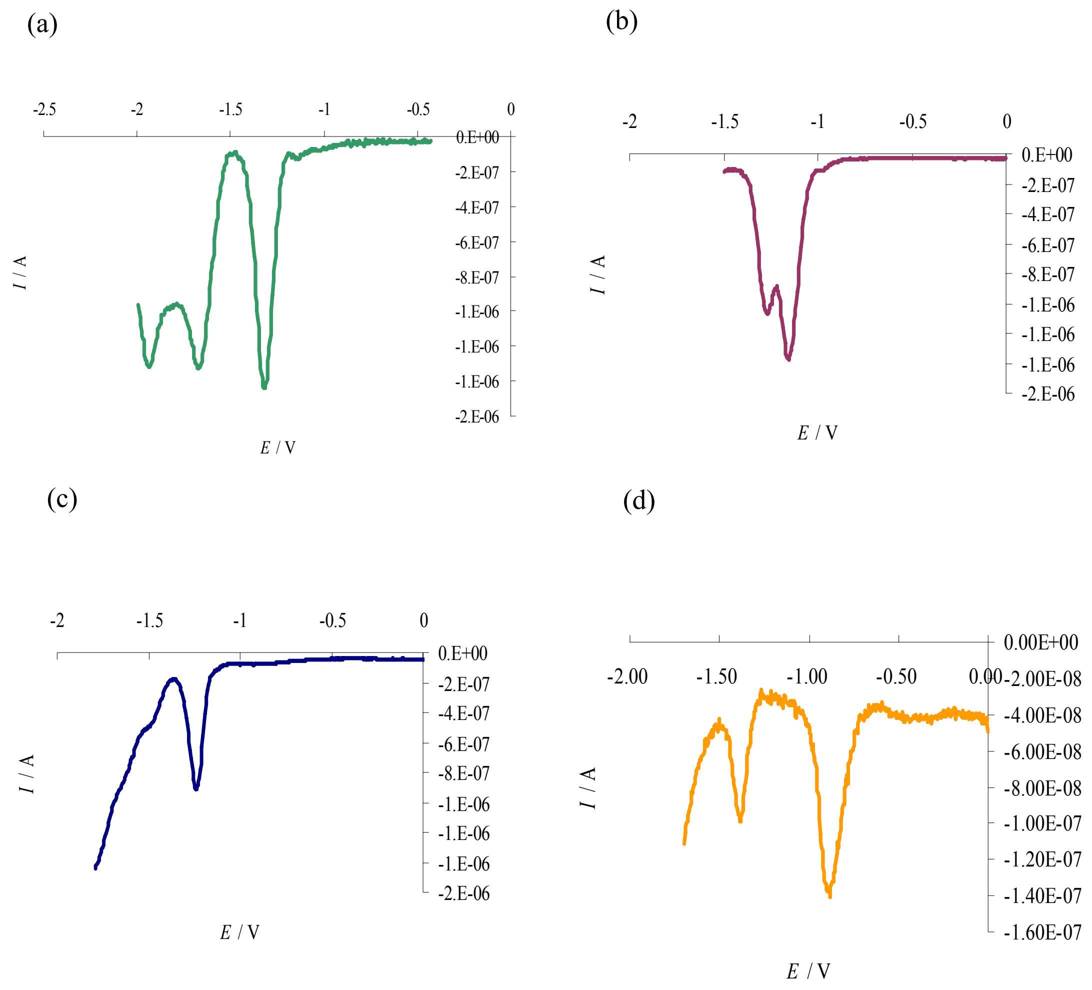

Figure S1. Differential pulse voltammograms of **1** (a), **2a** (b), **3a** (c) and **4** (d) in CH_2Cl_2. 0.1 M *n* -Bu_4NPF_6, Pt electrode, scan rate 100 mV s^{-1}, V vs SCE.

2. DFT calculations

B3LYP/6-31G(d) level using the Gaussian program

(a) (b)

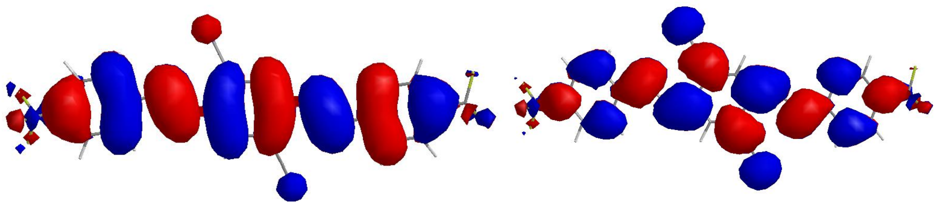

Figure S2. (a) HOMO orbital (6.42 eV) and (b) LUMO orbital (3.27 eV) of **1**.

(a) (b)

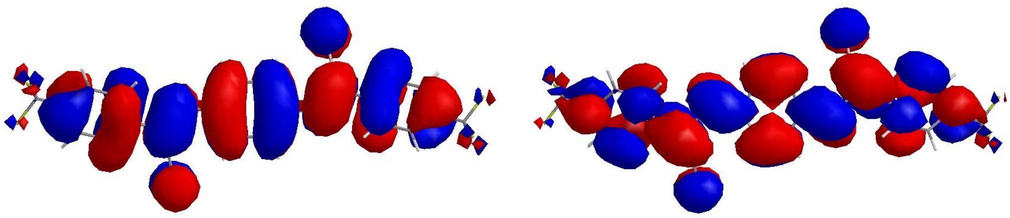

Figure S3. (a) HOMO orbital (6.34 eV) and (b) LUMO orbital (3.22 eV) of **2a**.

(a) (b)

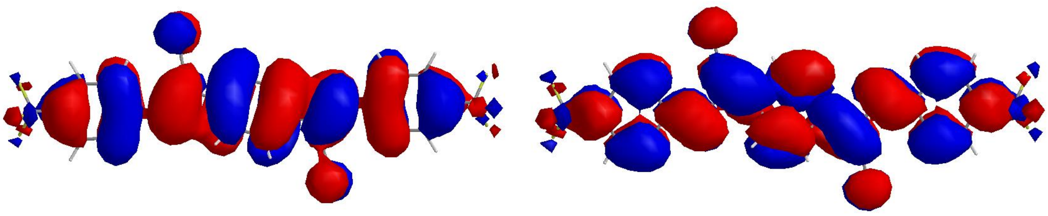

Figure S4. (a) HOMO orbital (6.53 eV) and (b) LUMO orbital (3.12 eV) of **3a**.

(a) (b)

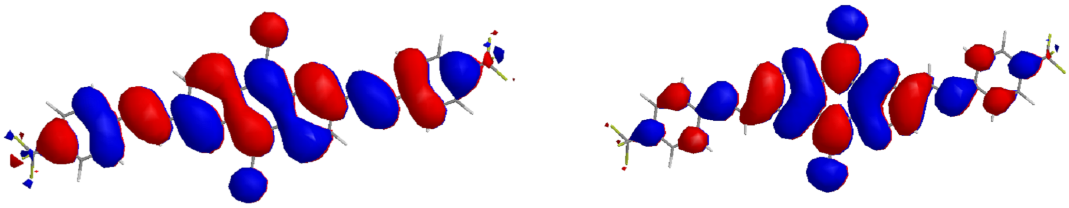

Figure S5. (a) HOMO orbital (6.07 eV) and (b) LUMO orbital (3.41 eV) of **4**.

(a) (b)

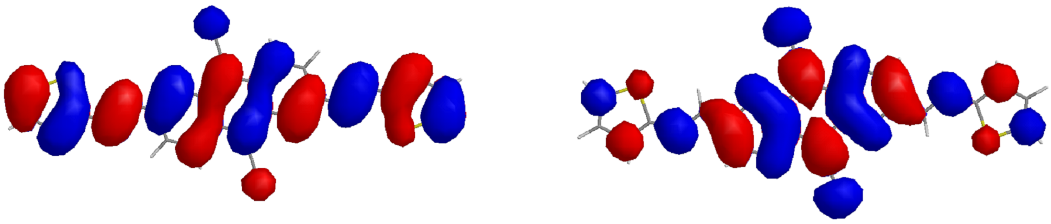

Figure S6. (a) HOMO orbital (5.50 eV) and (b) LUMO orbital (3.05 eV) of **5**.

(a) (b)

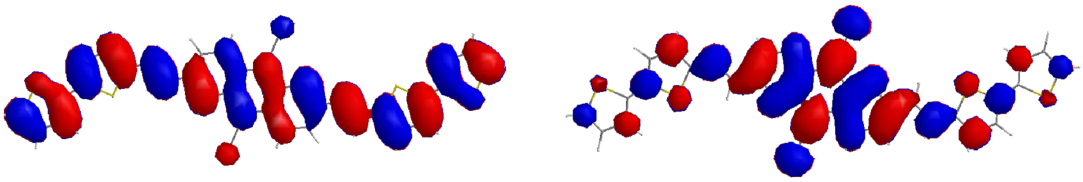

Figure S7. (a) HOMO orbital (5.24 eV) and (b) LUMO orbital (3.08 eV) of **6**.

3. FET characteristics

3-1. Bottom-contact devices

(a) (b)

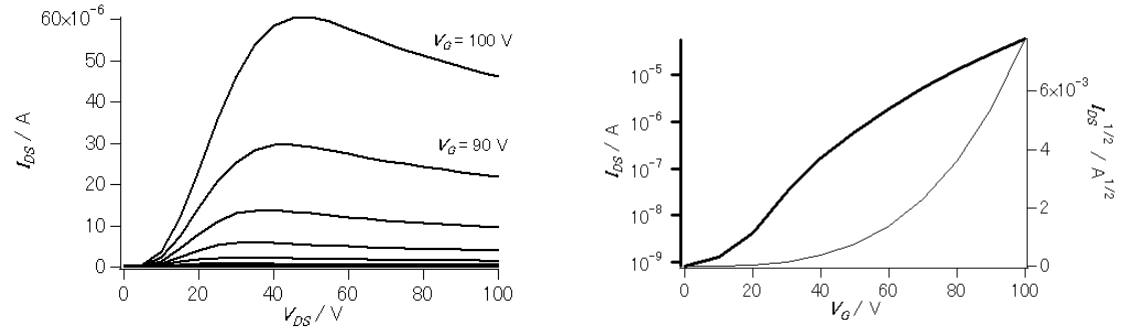

Figure S8. (a) Output characteristics of **1** and (b) transfer characteristics of **1** at a drain voltage of 50 V (T_{sub} = 50 °C, HMDS). The mobility calculated in the saturation regime is 6.6× 10^{-4} cm^2 V^{-1} s^{-1} (SiO_2: 300 nm, active layer: 50 nm, L/W = 25 µm/294000 µm).

(a) (b)

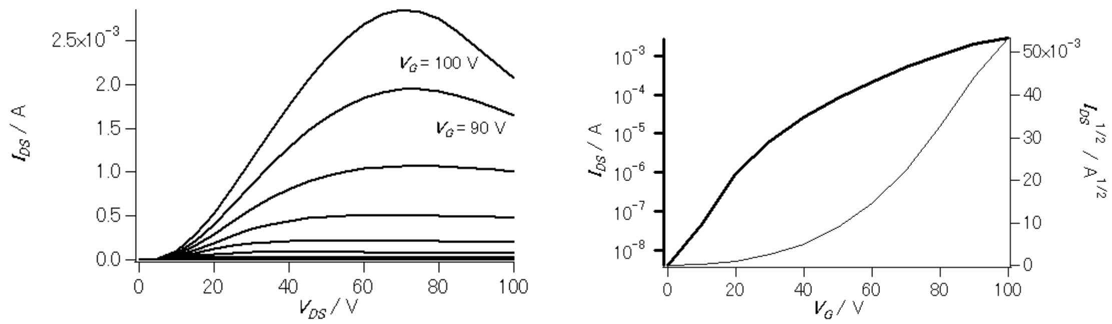

Figure S9. (a) Output characteristics of **2a** and (b) transfer characteristics of **2a** at a drain voltage of 70 V (T_{sub} = 50 °C, Bare). The mobility calculated in the saturation regime is 1.6×10^{-2} cm^2 V^{-1} s^{-1} (SiO_2: 300 nm, active layer: 50 nm, L/W = 25/294000).

(a) (b)

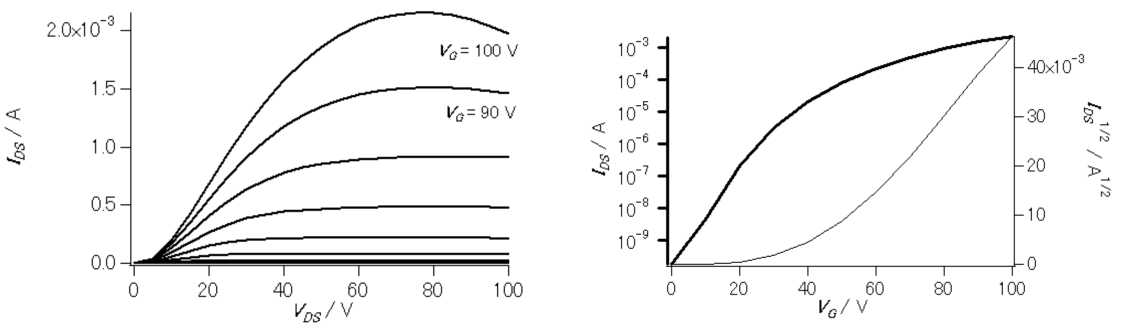

Figure S10. (a) Output characteristics of **2b** and (b) transfer characteristics of **2b** at a drain voltage of 75 V (T_{sub} = 20 °C, Bare). The mobility calculated in the saturation regime is 1.1× 10^{-2} cm^2 V^{-1} s^{-1} (SiO_2: 300 nm, active layer: 50 nm, *L*/*W* = 25/294000).

(a) (b)

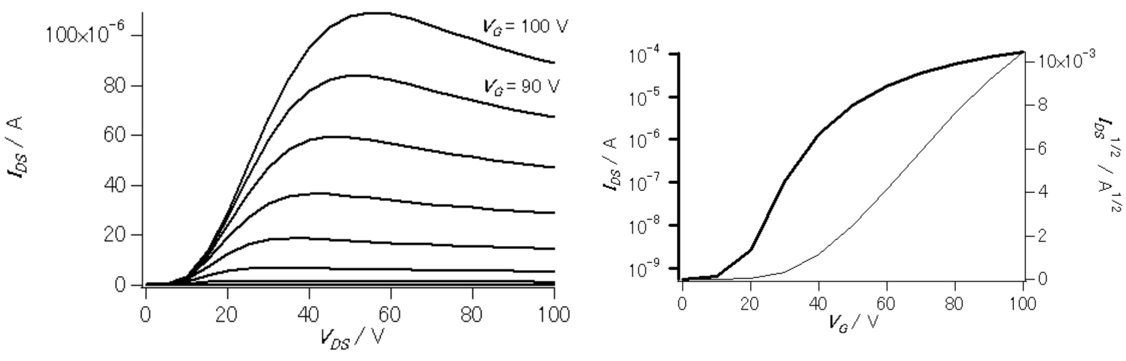

Figure S11. (a) Output characteristics of **3a** and (b) transfer characteristics of **3a** at a drain voltage of 55 V (T_{sub} = 20 °C, Bare). The mobility calculated in the saturation regime is 4.5×10^{-4} cm^2 V^{-1} s^{-1} (SiO_2: 300 nm, active layer: 50 nm, *L*/*W* = 25/294000).

(a)

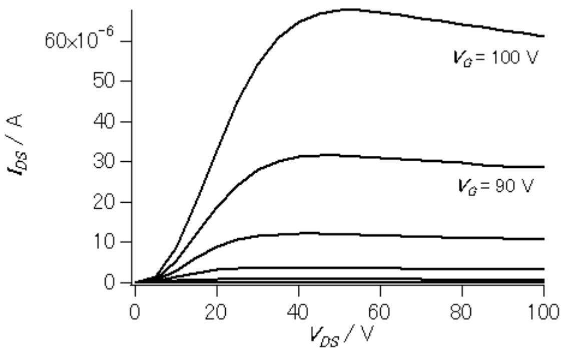

(b)

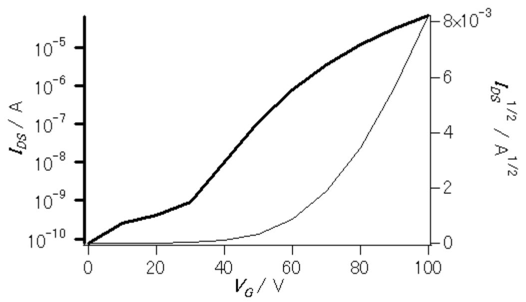

Figure S12. (a) Output characteristics of **3b** and (b) transfer characteristics of **3b** at a drain voltage of 50 V (T_{sub} = 50 °C, HMDS). The mobility calculated in the saturation regime is 9.2× 10^{-4} cm^2 V^{-1} s^{-1} (SiO_2: 300 nm, active layer: 50 nm, *L*/*W* = 25/294000).

(a)

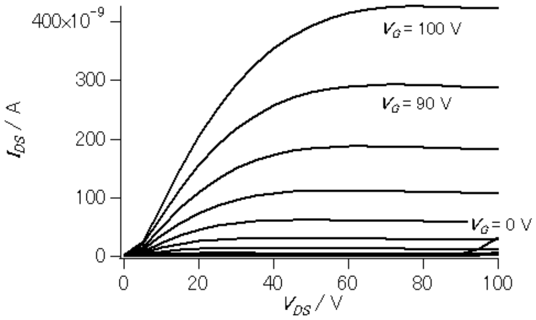

(b)

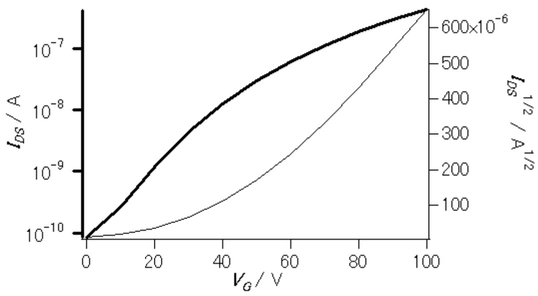

Figure S13. (a) n-Type output characteristics of **5** and (b) transfer characteristics of **5** at a drain voltage of 70 V (T_{sub} = 20 °C, HMDS). The mobility calculated in the saturation regime is 1.8× 10^{-6} cm^2 V^{-1} s^{-1} (SiO_2: 300 nm, active layer: 50 nm, *L*/*W* = 25/294000).

(a) (b)

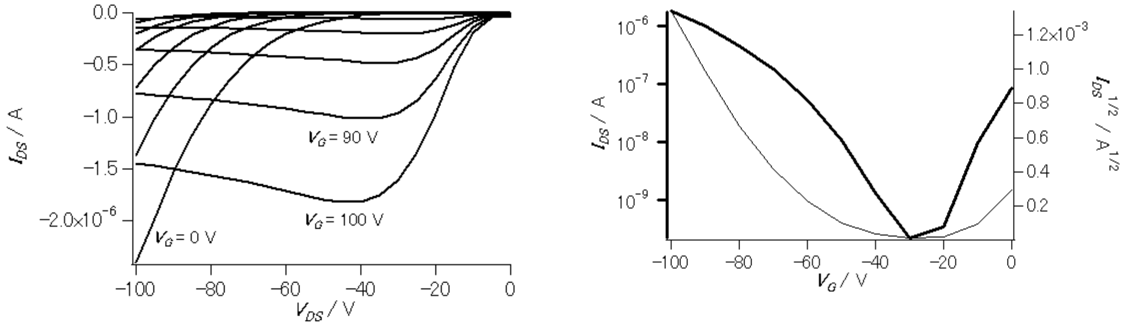

Figure S14. (a) p-Type output characteristics of **5** and (b) transfer characteristics of **5** at a drain voltage of 45 V (T_{sub} = 20°C, HMDS). The mobility calculated in the saturation regime is 1.2× 10^{-6} cm^2 V^{-1} s^{-1} (SiO_2: 300 nm, active layer: 50 nm, *L/W* = 25/294000).

(a) (b)

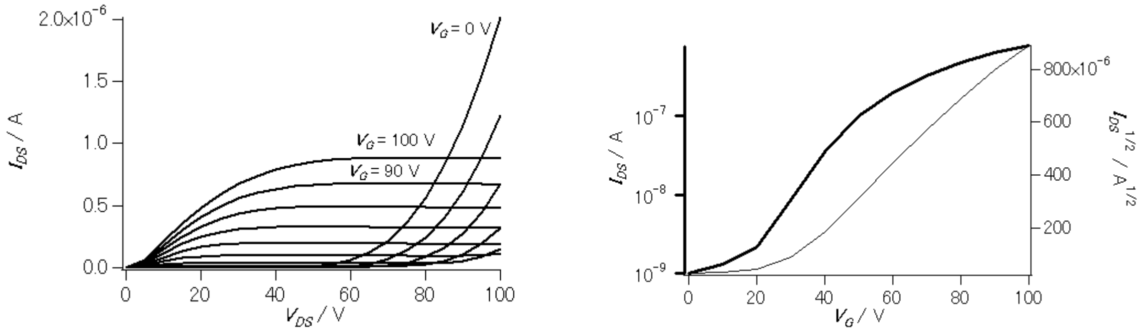

Figure S15. (a) n-Type output characteristics of **6** and (b) transfer characteristics of **6** at a drain voltage of 40 V (T_{sub} = 20°C HMDS). The mobility calculated in the saturation regime is 2.4× 10^{-6} cm^2 V^{-1} s^{-1} (SiO_2: 300 nm, active layer: 50 nm, *L/W* = 25/294000).

(a) (b)

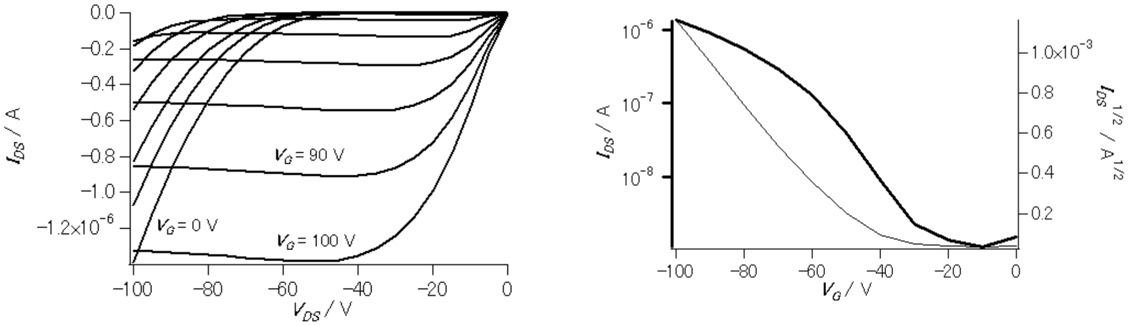

Figure S16. (a) p-Type output characteristics of **6** and (b) transfer characteristics of **6** at a drain voltage of 40 V (T_{sub} = 20 °C, HMDS). The mobility calculated in the saturation regime is 2.7× 10^{-6} cm^2 V^{-1} s^{-1} (SiO_2: 300 nm, active layer: 50 nm, L/W = 25/294000).

3-2. Top contact devices

(a) (b)

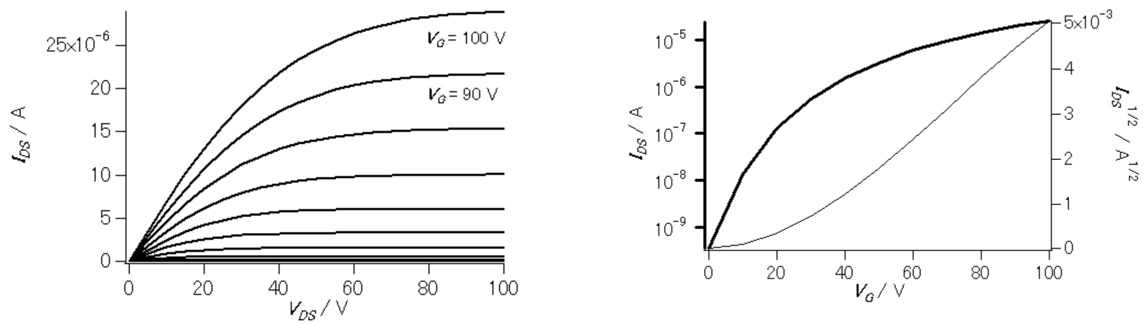

Figure S17. (a) Output characteristics of **2a** and (b) transfer characteristics of **2a** at a drain voltage of 55 V (T_{sub} = 20 °C, Bare). The mobility calculated in the saturation regime is 0.04 cm^2 V^{-1} s^{-1} (SiO_2: 200 nm, active layer: 30 nm, L/W = 50/1000).

Supplementary Material (ESI) for Journal of Materials Chemistry

3-3. Solution process

(a) (b)

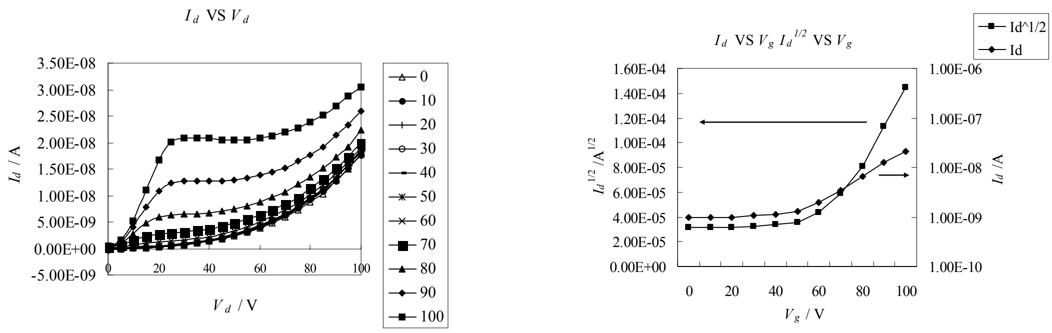

Figure S18. (a) Output characteristics of **2a** and (b) transfer characteristics of **2a** at a drain voltage of 30 V (annealed at 100 °C, Bare). The mobility calculated in the saturation regime is 1.5×10^{-7} cm^2 V^{-1} s^{-1} (SiO_2: 300 nm, L/W = 25/294000).

(a) (b)

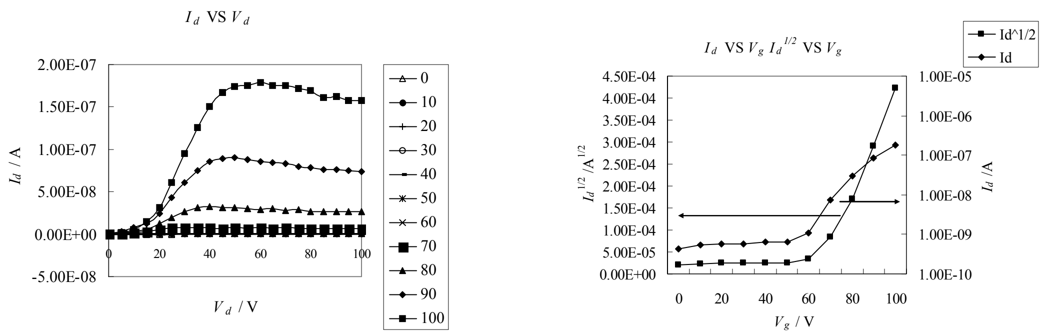

Figure S19. (a) Output characteristics of **3a** and (b) transfer characteristics of **3a** at a drain voltage of 60 V (annealed at 100 °C, Bare). The mobility calculated in the saturation regime is 2.1×10^{-6} cm^2 V^{-1} s^{-1} (SiO_2: 300 nm, L/W = 25/294000).

4. XRD patterns

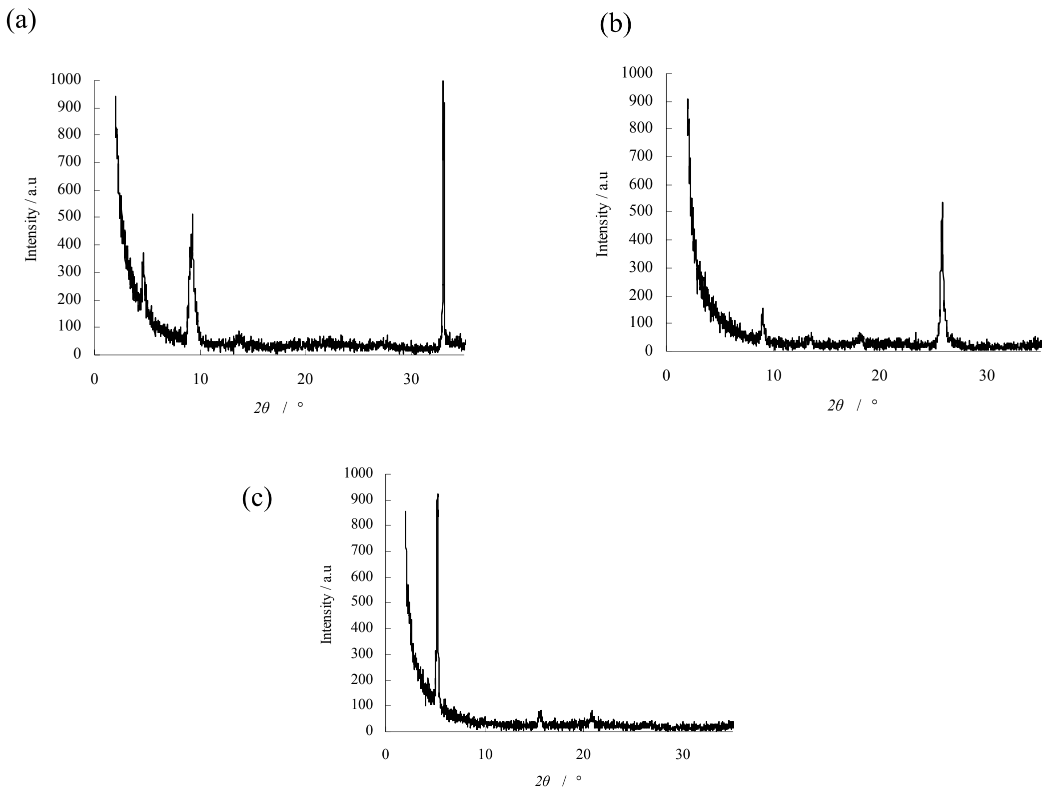

Figure S20. X-ray diffractograms of 50 nm films (a) for **1**, (b) for **4** and (c) for **5** deposited at 20 °C on untreated substrates.

Films of compound **2b**, **3b**, and **6** did not show XRD peaks.

5. AFM measurement

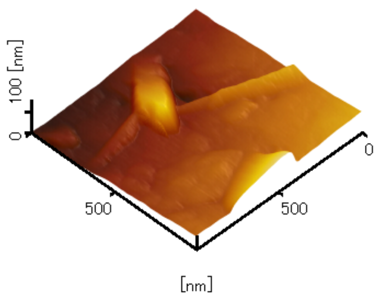

Figure S21. AFM image of a 50 nm film of compound **1** deposited at 20 °C on an untreated substrate.